System Dynamics Based Study on Fuel Cycle and Electric Power Balance during Deuterium-Deuterium Start-Up of a Tokamak Fusion Reactor

Yusuke YAMAZAKI, Kento MIYAMAE[1)] and Hiroshi YAMADA[1)]

Faculty of Engineering, The University of Tokyo, Bunkyo, Tokyo 113-8654, Japan

[1)]*Graduate School of Frontier Sciences, The University of Tokyo, Kashiwa, Chiba 277-8561, Japan*

(Received 27 May 2024 / Accepted 29 July 2024)

Start-up of a tokamak DEMO reactor using only deuterium (D) fuel without the initial loading of tritium (T) has been assessed from the aspect of fuel cycle and electric power balance. The temporal evolution of plasma parameters and electric power demands for current drive and BOP have been analyzed by means of system dynamics. One of the critical issues for a fusion DEMO reactor is securing the initial loading of T. While this "*DD start-up*" scenario would be a solution of this critical issue, this operation requires external energy input to maintain the burning plasma condition for several months until sufficient DT burning is established. The plasma temperature increases with the increase of α heating by the growth of T fraction. Consequently, the current drive power, hence, its electric power demand is reduced while the electric power generation increases. The positive net electric power output is anticipated well before the full DT operation is built up. Operational options to improve the performance and sensitivity of the performance to assumed parameters have been also discussed.

Keywords: fusion DEMO reactor, DD start-up, plasma current drive, fuel cycle, electric power balance

DOI: 10.1585/pfr.19.1405027

1. Introduction

Tritium (T), the fuel of the fusion reactor, is a scarce resource. It is pointed out that availability of T is limited to about 30 kg produced by heavy water reactors all over the world [1, 2]. Its significant amount will be consumed by ITER which does not accommodate T breeding [3] and the demand of T will expand due to CFETR in China [4] and other DT burning programs in emerging start-up companies such as SPARC [5]. A fusion DEMO reactor burns several hundred grams of T a day to produce several hundreds MW of net electric power. Without the issue of T availability, it would be reasonable that a DEMO reactor holds several kg of T inventory to secure operational margin and that similar amount of initial loading of T would be requested. Therefore, it is concerned that T availability restricts worldwide development of DEMO reactors. It should be also noted that transportation of T raises security concerns since T is radioactive. Securing of initial loading of T is a critical issue for feasibility of a DEMO reactor because of these reasons.

As an alternative solution, the start-up from only deuterium (D) fuel without the initial loading of T has been proposed [6]. This DD start-up scenario relies on DD reaction in the initial operational phase. The supply of T produced by the reaction of Li and neutrons generated from DD and DT reactions in the blanket increases the fraction of T in burning plasma and a steady state with a fuel DT ratio of 1:1 is reached consequently. It is noted that T production rate through DD reactions in the plasma is only in the order of 10^{-4} compared with this external T supply. The electric power generation by fusion power increases accompanied with this build-up. Because of the lower cross-section of DD reaction than of DT reaction, an external power input is required to maintain the temperature sufficient for the fusion burning conditions and to drive the plasma current for tokamak plasmas in this build-up phase.

The principle of this DD start-up scenario for a tokamak DEMO reactor has been examined by means of system dynamics [7, 8]. The problem of this scenario is that it takes several months to reach the DT steady-state. Towards the assessment of technical and economical feasibility of the DD start-up, the circulating electric power has been investigated together with the T fuel cycle in this study. The beneficial effects of an innovative scheme of direct internal recycling of fuels [9] and the amount of initial loading on acceleration of the build-up are also discussed.

2. System Dynamics of Fuel Cycle and Electric Power Balance

System dynamics is an analysis method to approach and solve the non-linear dynamics of complex systems. The basic concept is based on combination of stocks, flows

author's e-mail: yuteno0910@g.ecc.u-tokyo.ac.jp

and loops in a visual framework. In this study, the commercial system dynamics software *"Stella Architect"* [10] was used.

The present model of a system dynamics basically follows the previous study [8]. The shapes of temperature T and electron density n_e profiles are fixed as

$$T(\rho) = T_0(1-\rho^2)^{1.5}, \tag{1}$$

and

$$n_{\mathrm{e}}(\rho) = n_{\mathrm{e},0}(1-\rho^2)^{0.6}. \tag{2}$$

The ion and electron temperatures are set to the same. Temporal evolution of temperature is calculated from the power balance between heating power and the losses due to radiation and energy confinement while electron density is fixed in time. DD and DT fusion reactions are considered with taking account of enhancement due to high energetic D from NBI and T from DD reaction while D^3He reaction is not considered because of its negligible effect. Heating power includes auxiliary external heating and collisional heating due to all energetic particles such as α produced by fusion reactions in DT plasmas. Bremsstrahlung, synchrotron radiation and line radiation due to impurities represented by Ar are involved in radiation losses. The parameters given in the JA DEMO study [12] are used in this study (see Table 1). The parametric dependence of the energy confinement time is assumed as the tokamak H-mode scaling (ITERH-98P(y,2) [11]) with a supplemental enhancement factor. Particle confinement time of T is set as 1.5 times the energy confinement time. The profiles of plasma properties are analyzed in 7 shells along the minor radius. The diffusive transport of He ash is calculated in the shell structure. Particle confinement time of He is adjusted to match the concentration level given by the DEMO design study (particle confinement time of He is 2.25 times the energy confinement time). While the shape of profile of impurity ions (Ar) is assumed to be Eq. (2), D and T fuel ions are assumed to take the same shape of profiles and they are determined to fulfill charge neutrality under the given total particle balance in the T cycle. Here the SOL-divertor region and plasma vacuum vessel have not been incorporated in the model as stocks. This treatment approximates 100 % of recycling. Details of the model of tritium cycle configured by its production in the blanket and flow/stock/loss through related components are described in [7, 8]. The tritium breeding ratios (TBRs) are set as 1.1 and 0.67 for DT and DD reactions, respectively.

Sustainment of toroidal plasma current is prerequisite for a tokamak reactor. External current drive is inevitable since spontaneous bootstrap current is not sufficient to keep the required current. The JA DEMO design study has indicated that 62 MW of NBI is needed to keep the plasma current of 14.0 MA with the bootstrap fraction of 0.59 [12]. These values are estimated under the steady state condition, therefore, more power is required in the build-up phase of the DD start-up operation because of lower temperature than in the targeted steady state. Hence the electric power demand for the external current drive is a critical factor in the electric power balance of the plant. The major element of this study is to develop a plasma current model in conjunction with the tritium cycle in the DD start-up scenario. The electric power required for the balance of plant (BOP) is also evaluated consistently.

Table 1 Used reference parameters from JA DEMO [12]. Parameters from 1 to 9 are used in calculation and parameters from 10 to 12 are referred for the benchmark.

parameters	value	units
1. Major radius (R)	8.20	m
2. Minor radius (a)	2.39	m
3. Safety factor (q)	5.3	-
4. Toroidal magnetic field (B_{p})	6.90	T
5. Volume averaged density	5.27×10^{19}	m^{-3}
6. Plasma current (I_{p})	14.0	MA
7. Confinement enhancement (HH_{98y2})	1.47	-
8. Fraction of He	0.041	-
9. Fraction of Ar	0.0026	-
10. External current drive power	61.9	MW
11. Fusion power (P_{f})	1403	MW
12. Bootstrap current fraction (f_{BS})	0.59	-

3. Integration of Current Drive and Tritium Cycle

The model of the required power for current drive is integrated consistently with the temporal development of plasma parameters under the tritium cycle. In general, bootstrap current is not sufficient to generate all the required plasma current and it is presumed that NBI current drive covers a shortage of the current. The total plasma current I_{p} is given by the sum of I_{BS} and I_{NBI}. The input power of NBI dissipates in the plasma and works for plasma heating.

Poloidal magnetic field is needed to estimate the bootstrap current I_{BS}. The poloidal magnetic field was obtained by Maxwell's equations as follow:

$$B_{\mathrm{p}}(\rho) = \frac{\mu_0}{2\pi a\rho}\int_{S(\rho)} J_{\mathrm{p}}\,\mathrm{d}S, \tag{3}$$

where ρ is the normalized minor radius ($0 \leq \rho \leq 1$), μ_0 is the permeability of vacuum, J_{p} is the plasma current density (total of bootstrap current and the current driven by NBI), S is the area of a circle of radius $a\rho$. This simple cylindrical evaluation is adjusted by multiplying a factor to match the safety factor q in the design study [12].

Bootstrap current density J_{BS} [A m^{-2}] is calculated by

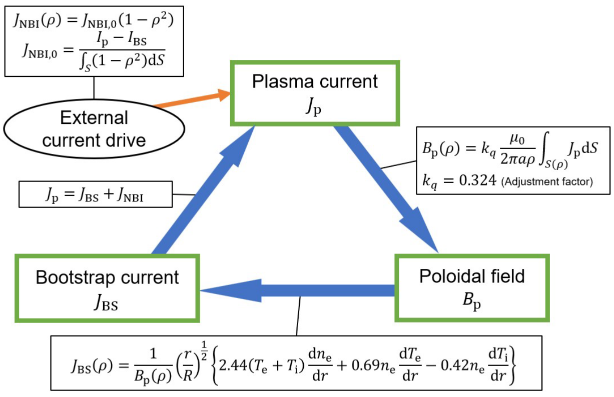

Fig. 1 Schematic diagram of the relationship between plasma current, Bootstrap current, and poloidal magnetic field.

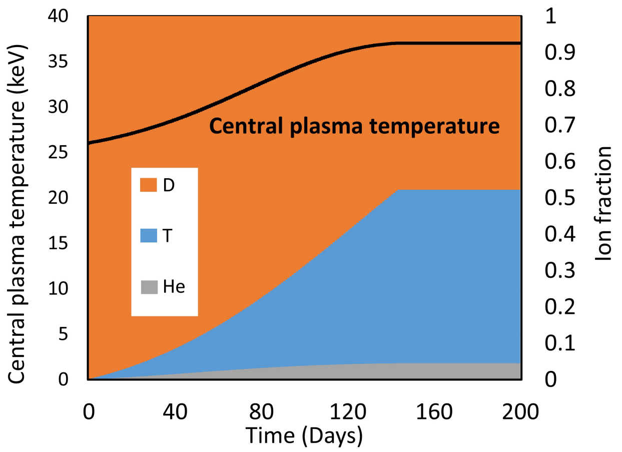

Fig. 2 Black solid line ("Plasma center temperature") shows the temporal evolution of the central plasma temperature and fraction of ions. Filled colors show the fraction of each ion, which are D in orange, T in blue, and He in gray.

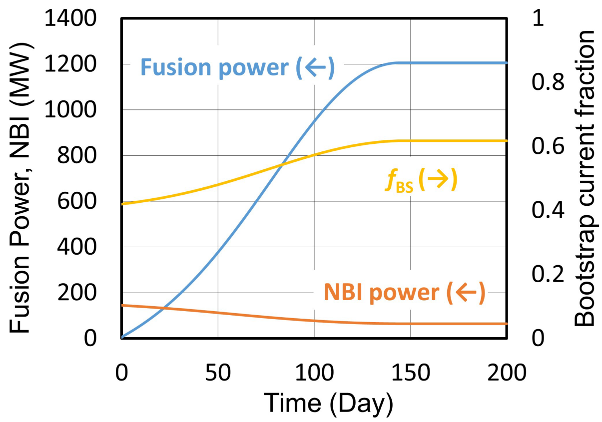

Fig. 3 Temporal evolutions of fusion power [MW] in blue, NBI power [MW] in orange, and bootstrap current fraction in yellow.

the following model [13, 14]:

$$J_{\rm BS} = \frac{1}{B_{\rm p}(\rho)}\left(\frac{r}{R}\right)^{\frac{1}{2}}\{3.91(T_{\rm e}+T_{\rm i})\frac{\mathrm{d}n_{\rm e}}{\mathrm{d}r} + 1.11n_{\rm e}\frac{\mathrm{d}T_{\rm e}}{\mathrm{d}r} - 0.67n_{\rm e}\frac{\mathrm{d}T_{\rm i}}{\mathrm{d}r}\}, \quad (4)$$

where r is the minor radius variable $a\rho$ [m], $T_{\rm e}$ and $T_{\rm i}$ are the temperatures of electrons and ions [eV], and $n_{\rm e}$ is the electron density [$10^{19}\mathrm{m}^{-3}$]. The derivative term in Eq. (4) is obtained by differentiating Eq. (1) and Eq. (2) by r.

The current drive efficiency of NBI [A/W] is calculated by the following model [15, 16]:

$$\frac{I_{\rm NBI}}{P_{\rm NBI}} = \frac{0.06T_{\rm e}}{n_{\rm e}R\times 10^{-20}}\left(\frac{1}{Z_{\rm b}} - \frac{1}{Z_{\rm i}}\right), \quad (5)$$

where $Z_{\rm b}$ and $Z_{\rm i}$ are the effective charges of the beam and plasma, respectively. The charge of beam is 1 and $Z_{\rm i}$ is calculated from the fraction of ion species. Here $T_{\rm e}$ is the electron temperature in keV.

The plasma current density driven by NBI $J_{\rm NBI}$ is assumed to take the parabolic $(1-\rho^2)$ profile. The procedure to get consistent plasma current profile is described in Fig. 1. The bootstrap current is calculated first and then the NBI driven current compensates the shortage of current, $I_{\rm NBI}(= I_{\rm p} - I_{\rm BS})$, with the parabolic current distribution. Then poloidal field by the constructed plasma current profile and consequent $J_{\rm BS}$ are recalculated. This process is iterated to get converged results.

Figure 2 shows the temporal evolution of the central plasma temperature and fraction of ions. This study pays attention to the timescale of tritium cycle and build-up of tritium fuels while the current ramp-up phase in much shorter timescale than this timescale is out of scope. In this reference case, it takes 144 days to establish DT steady state where the DT ratio is 1:1. The central plasma temperature starts at 26.0 keV and becomes steady at 37.0 keV. Figure 3 shows the temporal evolution of fusion power [MW], NBI power for current drive [MW], and bootstrap current fraction $f_{\rm BS}$. The NBI power required to drive 14.0 MA current starts at 145 MW and settles down to 64.4 MW at the DT steady state. Compared with this 145 MW of NBI power in the initial phase, the heating power from DD reactions is as small as 3.1 MW (2.4 MW between two thermal D's and 0.7 MW between thermal D and D beam). The significantly high current drive power is needed until the temperature reaches the targeted values at the DT steady state. The bootstrap fraction $f_{\rm BS}$ starts at 0.42 and reaches 0.62 at the DT steady state. The benchmark comparison of these parameters obtained by the system dynamics simulation with those from sophisticated physics design study [12] has shown reasonable agreement and it can be concluded that the present model is validated.

Figure 4 shows plasma current density at the DT steady state. Bootstrap current takes a hollow profile as expected from pressure gradient and poloidal field profiles, and NBI driven current is assumed to take a parabolic profile which is realized by flat profile of deposited power.

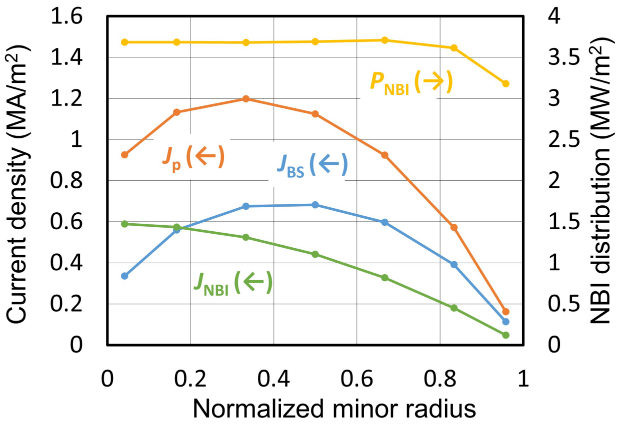

Fig. 4 Current density profiles of bootstrap current (“J_{BS}”) in blue, NBI driven current (“J_{NBI}”) in green and total plasma current (“J_p”) in orange when the DT steady state is achieved. NBI heating power distribution (“P_{NBI}”) in yellow.

4. Electric Power Balance in Plant

In order to operate a tokamak fusion reactor as a plant, electric power demand for peripheral equipment (BOP, Balance Of Plant) is inevitable in addition to plasma heating/current drive power. In this study, the cooling system and the cryogenic system have been considered since they are major BOP with particularly high electric power consumption.

4.1 Cooling system

The cooling system is used to cool components, which manage a massive amount of heat, such as blanket, divertor, and plasma heating devices. The cooling system of JA DEMO is assumed to have the same specifications as the cooling system of PWR (Pressurized Water Reactor), which uses water as coolant. The model of the cooling system has been built on the basis of the previous work on cooling systems in fusion reactors with 1.5 GW of fusion power [17], and the required cooling capability and electric power demand have been evaluated for blanket, divertor, vacuum vessel, back plate, and NBI.

The divertor is cooled by the two types of cooling systems. These two have different coolant pipe materials to manage corresponding heat removal capability. The first is a Cu-alloy (CuCrZr) system. Because of its high thermal conductivity, CuCrZr is used for cooling water pipes for divertor target plates exposed to particularly high heat flux from the plasma. The second is the RAFM (Reduced Activation Ferritic Martensitic) material system. RAFM materials have high tolerance against neutron load although thermal conductivity is inferior to Cu-alloy. They are used for divertor components with moderate heat load. The RAFM material system is connected to the same cooling system as the blanket, while the Cu-alloy material system has its own cooling system. The vacuum vessel and back plate are also connected to one cooling system.

Table 2 Amount of heat removal for each component and the power consumption required for heat removal in a fusion reactor with 1500 MW of fusion power [17].

Component	Device	Power
Blanket	Primary pump	19.6 MW
(1574 MW)	Primary PVCS	2.8 MW
	Primary pressurizer	4.8 MW
	Secondary pump	4.1 MW
	Secondary PVCS	2.8 MW
	Secondary pressurizer	1.1 MW
	Turbine system	15.2 MW
Divertor (RAFM)	Pump	2.5 MW
(291 MW)	PVCS	2.8 MW
	Pressurizer	1 MW
Divertor (Cu-alloy)	Primary pump	5.4 MW
(172 MW)	Secondary pump	0.2 MW
	PVCS	0.7 MW
Back plate	Pump	0.1 MW
(16 MW)	Heater	2.6 MW
Vacuum vessel	PVCS	0.7 MW
(0.043 MW)	Final pump	3 MW

The main power-consuming devices in the cooling system are cooling water pumps, pressurizers, cooling water purifiers (PVCS:Purification Volume Control Systems), and heaters. Since the flow rate of the cooling water is proportional to the amount of heat exhausted [17], the power consumed by the pumps and PVCS was assumed to be proportional to the fusion power. The power consumption of the pressurizers and heaters is assumed to be constant at the design value regardless of fusion power, and that of the turbine system is assumed to be proportional to the amount of electricity generated. The amount of heat to be removed from each component except for NBI P_{comp} has been evaluated using the fusion power P_f and the estimate in the previous study [17] P_{data} as follows:

$$P_{comp} = \frac{P_f}{1500\,\mathrm{MW}} \times P_{data}. \quad (6)$$

Table 2 shows the amount of heat removal for each component and the power consumption required for heat removal in a fusion reactor with 1.5 GW of fusion power [17]. Another device that needs to be cooled are NBI. Required heating and current drive capability of NBI is evaluated as described in the previous section. The electric power-to-beam conversion efficiency in NBI is assumed to be 0.5 [12]. The power required to cool the heat generated as energy loss has been evaluated along with the analogy to divertor Cu-alloy cooling system since these two are in the similar heat-load environment. The efficiency of 6.3 MW/172 MW in the cooling efficiency of divertor Cu-alloy cooling system has been used for the cooling efficiency of NBI cooling system.

The role of the cooling system is not only to cool equipment. It also plays an essential role in generating electricity using the heat removed from the equipment. The cooling system of a blanket-divertor (RAFM) has a power generation system, and the amount of electricity generated is proportional to the amount of heat exhausted from these components. The heat to electricity conversion efficiency is set at 0.33 which is derived from the previous study (620 MW/1865 MW) [17].

4.2 Cryogenic system

Since the cryogenic system of JA DEMO would have configuration and requirement similar to ITER, the specification in this study is extrapolated from that in ITER. Extrapolation is simply proportional to the volume of the main body of a reactor. The power consumption by the cryogenic system in ITER is evaluated to be 35 MW [18]. Therefore, the power consumption is given by

$$P_{\mathrm{cryo}} = 35\,\mathrm{MW} \times \left(\frac{R}{R_{\mathrm{ITER}}}\right)^3, \tag{7}$$

$$\sim 81\,\mathrm{MW}, \tag{8}$$

where the major radius of ITER R_{ITER} is 6.2 m.

4.3 Result of electric power balance

Figure 5 shows the consequent temporal evolution of electric power balance, which corresponds to the reference case shown in Fig. 2. Here the electric power demand of NBI is double the required current drive power since the beam generation efficiency of NBI is assumed to be 0.5 [12]. It should be noted that this efficiency is challenging [19] with incorporation of a photo-neutralizer cell [20].

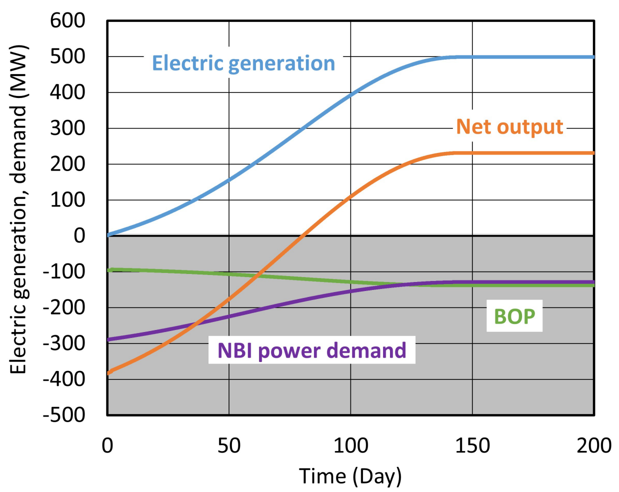

Fig. 5 Temporal evolution of electric power generation in blue, electric power demands of BOP in green and NBI in gray, and resultant net electric power power in orange in the reference case shown in Fig. 2. The negative value means consumption while positive value is generation.

With further innovation of a NBI system, the total performance of DEMO would be significantly enhanced. The electric power demand of BOP, the expected electric power generation and resultant net electric power output which can be delivered to the grid are also shown.

Electric power demand in the BOP starts at 96 MW and gradually increases with the increase of fusion power output up to 138 MW while that in the NBI starts at 290 MW and gradually decreases with the increase of plasma temperature, which mitigates required current drive power, down to 129 MW. The electric power generation at steady state is 498 MW. Thus, the resultant net electric output is negative in the build-up phase. At the beginning of operation 384 MW of external input of electric power is required in total and decreases as fusion output increases. Then electric power generation compensates the circulating power in the plant and the net output electric power stabilizes at 231 MW. It takes 80 days to get the net electrical output to become positive, which means that the DEMO becomes free-standing. The external input electric energy, which is a time integral of negative net output energy, of 413 GWh and it takes 98 days after the net output electric power becomes positive to recover this prior investment of electric energy.

5. Operational Scenario Options

The reference case discussed in prior sections is a conservative example and there can be a variety of operational options to improve the performance. Also, the sensitivity of performance to assumed parameters is of importance in elaboration of operational scenario and planning of related research and development. Here 4 options of incorporation of direct internal recycling, initial loading of T, NBI power constraint, and TBR are assessed referring to the reference case.

5.1 Direct Internal Recycling (DIR)

The reference model assumes that the fuel exhausted from the plasma is separated into deuterium and tritium, which are then refueled to the plasma. This circulation process consists of the stock in exhaust (ex), isolation (is) and fueling (fu) in the model (see Fig. 6). The timescale of this process is more than one hour in total. Innovative idea to shorten this cycle is Direct Internal Recycling (DIR) [9] by bypassing the exhaust system and the fueling system (see Fig. 6). Exhaust fuels are refueled directly without separation of DT and here it should be noted that He ash and impurities are screened out in this process. In this study, the time constant is assumed to be 100 s, which is a combination of the time constant of 60 s in the exhaust system and the time constant of 40 s in the fueling system [21]. The time constant of the exhaust system was obtained by dividing the vacuum chamber capacity by the effective vacuum pumping rate and that of the fueling system is evaluated from the experience of pellet injection with the screw-type

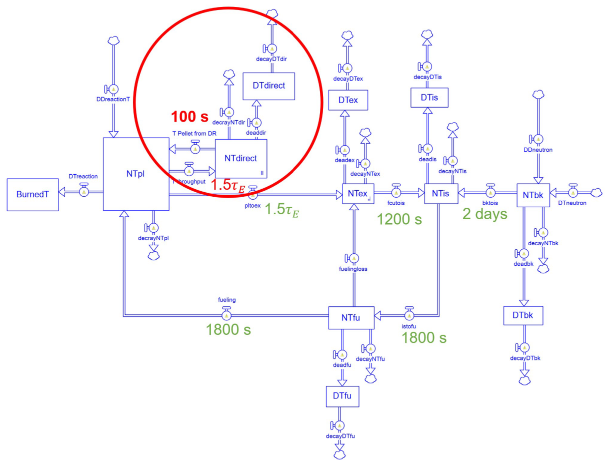

Fig. 6 Fuel cycle model with DIR in *Stella*. The area circled in red refers to the DIR model. Time constants between stocks used in the simulation are also described. Since the time constant from the fuel storage system NTfu to plasma NTpl includes the extraction process and the conductance between these stocks, it is much longer than the time constants described in the DIR.

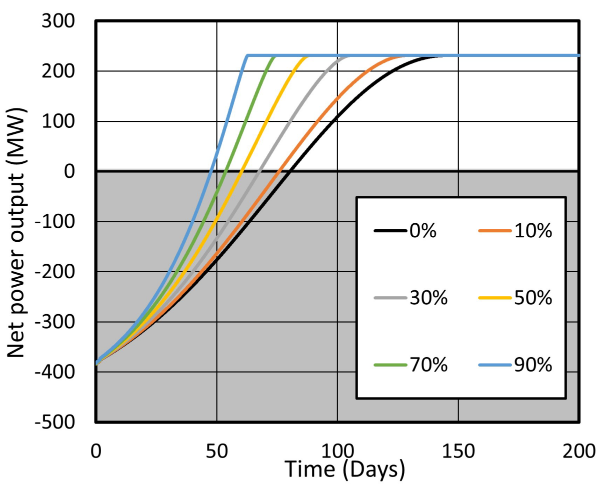

Fig. 7 Temporal evolution of net electric output for the reference case in black line (no DIR) and cases with different DIR ratios of 10 %, 30 %, 50 %, 70 % and 90 %.

solid hydrogen generator used in LHD [22]. The performance of this system is insensitive to this time constant. Even the reduction of the time constant to 20 s from 100 s makes a tiny difference in the result.

Figure 7 shows the temporal evolution of net electrical output to the grid with different DIR ratio, which is the ratio of the inflow to DIR to the total outflow from the plasma. It can be seen that the introduction of DIR significantly reduces the number of days to get positive net electrical output and that to reach the DT steady state as well. The period can be halved by 90 % of the DIR ratio. Consequently the total external input electric energy until the net electric output becomes positive can be also

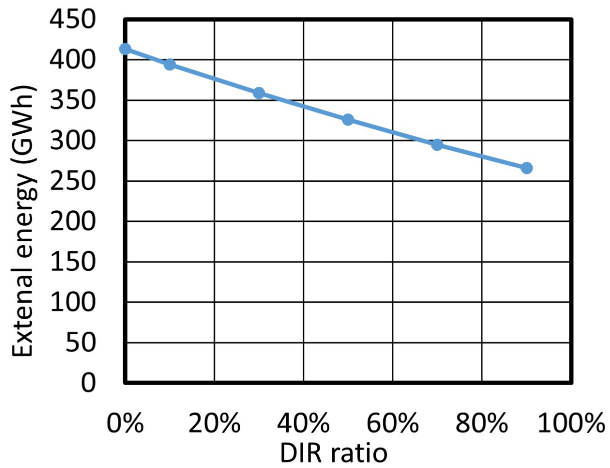

Fig. 8 Total amount of external input electric energy until net electrical output becomes positive as a function of the ratio of DIR.

reduced from 420 GWh to 270 GWh in the comparison of cases with 0 % and 90 % of the DIR ratios (see Fig. 8).

The DIR promotes tritium breeding by shortening the fuel cycle. The required specification of DT isolation system can be also mitigated and the amount of T in the fuel stock (“fu” in Fig. 6), which is controllable T inventory, increases effectively with reduction of uncontrollable T inventory in stocks other than “fu”. After 200 days of operation, the controllable T inventory is 1.7 kg in the case of the DIR ratio of 90 % compared with 0.25 kg in the case without DIR while the uncontrollable T inventory is reduced from 0.6 kg to 0.4 kg. While the increase of the DIR ratio seems to be preferable, it should be noted that the DIR ratio is limited by controllability of D. Under the present condition of simulation, too much supply of D from the DIR requires selective pumping/extraction of D from the plasma to keep the particle balance. The DIR ratio must be limited to less than 94 % to secure practical particle control.

5.2 Initial loading of tritium

In the reference case, the initial loading of T is set at zero. The effective start-up is anticipated if the initial loading of T is available. Therefore the effect of the amount of the initial loading of T has been investigated. The present scenario when the initial loading T is available assumes that T is fueled so that the DT ratio of 1:1 could be maintained until the initial loading T runs out. Figure 9 shows the temporal evolution of net electrical output with different amount of initial loading of T. Several hundred grams of T as initial loading accelerate the process significantly. If the initial T loading of just over 0.3 kg is available, the generated electric power can cover entire circulating electric power in the plant from the beginning of the operation. The initial T loading of 0.7 kg can maintain the DT steady state from the beginning. The effectivity of the initial load-

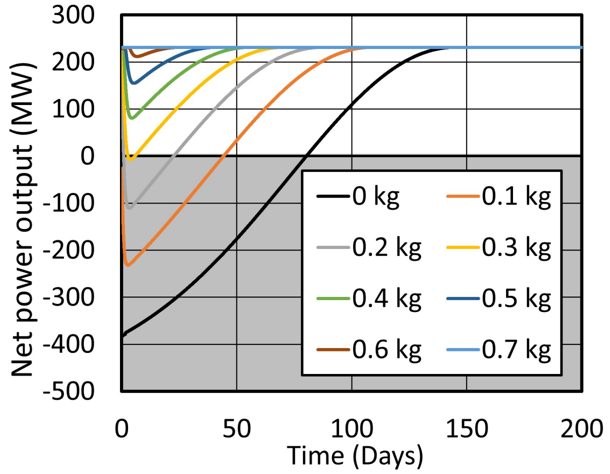

Fig. 9 Temporal evolution of net electric output for the reference case in black line ("Ref") (no DIR) and cases with 0.1 kg, 0.2 kg, 0.3 kg, 0.4 kg, 0.5 kg, 0.6 kg and 0.7 kg of initial T loading, respectively.

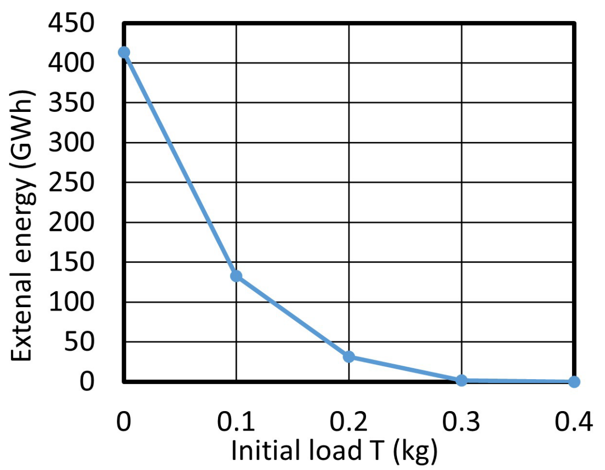

Fig. 10 Total amount of external input electric energy until net electrical output becomes positive as a function of the amount of the initial T loading.

ing of T on the required external input of electric energy is seen in Fig. 10. The initial T loading of even 100 g reduces the external input energy by a factor of 3 compared with the case without the initial loading of T.

5.3 NBI power constraint

According to the reference model, the maximum NBI power required for current drive at the beginning of the operation is about 150 MW. This specification would be technologically feasible from the ITER technology (up to 50 MW). However, mitigation of the requirement of NBI power is an important issue from the aspect of technology as well as economy. Therefore, the scenario with an upper limit of 100 MW for NBI has been investigated as a Ref. [23]. This power is not enough to drive 14.0 MA of plasma

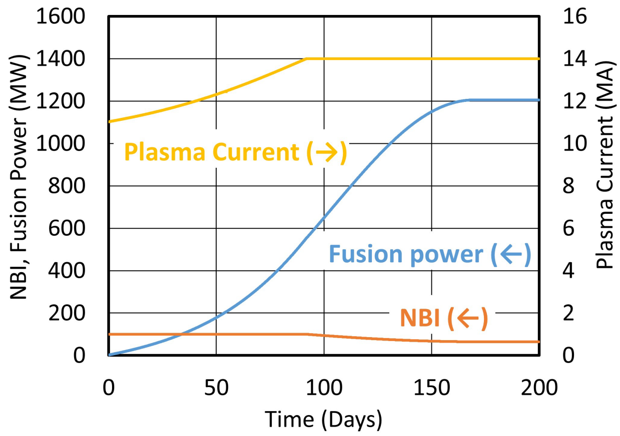

Fig. 11 Temporal evolution of plasma current in yellow, fusion power in blue and NBI power in orange when the NBI power is limited to 100 MW.

current in the initial phase where electron temperature is not high enough. While the plasma current is assumed to be a constant at 14.0 MA in the reference model, the plasma current is treated as a variable parameter which can be driven by the NBI power at the maximum of 100 MW in this scenario. Since the resultant achievable plasma current is smaller than the nominal designed value (14.0 MA), energy confinement time becomes shorter than the case of the full current and consequently evolution of plasma temperature becomes slower than the reference case.

Figure 11 shows the temporal evolution of plasma current, fusion power, and NBI power. The plasma current starts at 11.0 MA and reaches a steady state at 14.0 MA in 92 days. The number of days to reach the DT steady state increases to 170 days which is longer than the reference case by 26 days.

Figure 12 shows the temporal evolution of the power generation, power demands of BOP and NBI, and resultant net electrical output to the grid. The demand of the BOP starts at 94 MW and stabilizes at 138 MW, while the power demand in the NBI starts at 200 MW and stabilizes at 129 MW. The required external input at the beginning is reduce to 293 MW from 384 MW in the reference case. This scenario reaches the same DT steady state as the reference case (231 MW of net electric power output) at the end while it takes 106 days for the net electrical output to become positive (delayed by 26 days from the reference case). The amount of external input electric energy until the net electricity is positive is 496 GWh, which is larger than the reference case by 83 GWh. The limitation of the maximum current drive power and required external input energy are in trade-off relation.

5.4 Effect of TBR

The effect of TBR for DT has been also investigated. Figure 13 shows the numbers of required operational days

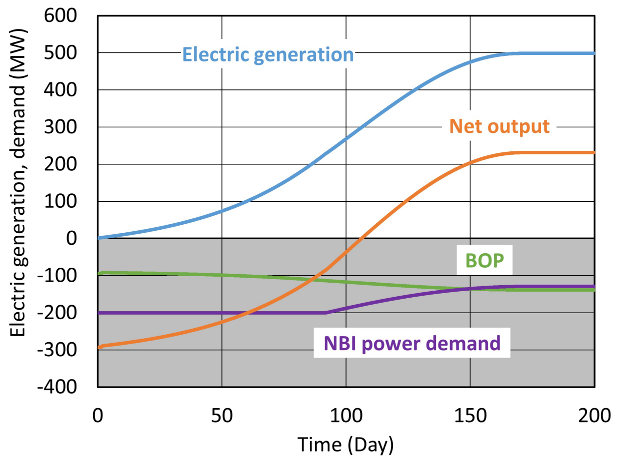

Fig. 12 Temporal evolution of electric power generation in blue, electric power demands of BOP in green and NBI in gray, and resultant net electric power power when the maximum NBI power is limited to 100 MW. The negative value means consumption while positive value is generation.

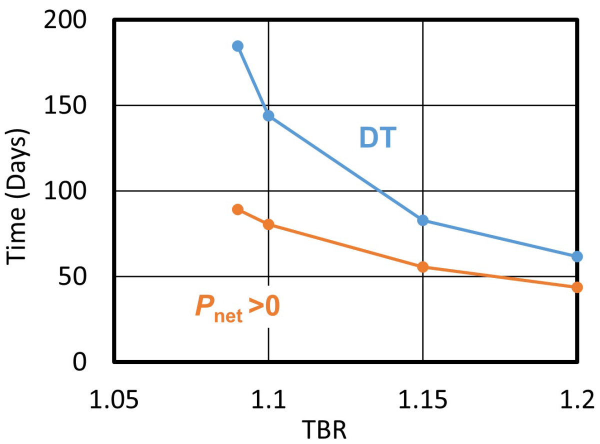

Fig. 13 The numbers of required operational days to reach the DT steady state in blue and to get positive net electric power output in orange as a function of TBR. TBR in the reference case is 1.1.

to reach the DT steady state in blue and to get positive net electric power output in orange as a function of TBR. Figure 14 shows the effect of TBR on the required external input electric energy. Improvement from 1.1 to 1.15 of TBR reduces required external input energy by 30 %.

As a derivation from the reference case, it has been found that the build-up of T concentration seriously slows down for TBR < 1.09. When TBR = 1.08, T ratio stays at 0.465 even after 500 days. This requirement of TBR is challenging in accordance with the target value of 1.05 in the development of JA DEMO blanket [24]. This constraint can be mitigated by the introduction of DIR. When the DIR ratio is 60 %, the DD start-up can be completed in 194 days with TBR of 1.05. This is pronounced evidence

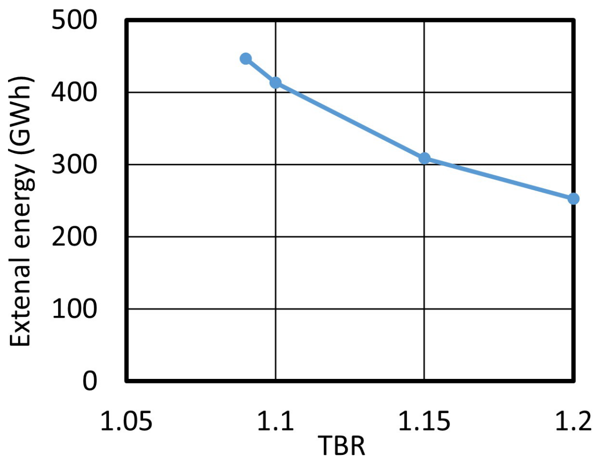

Fig. 14 Total amount of external input electric energy until net electrical output becomes positive as a function of TBR.

to show the advantage of DIR in DEMO.

6. Discussions and Conclusions

The present study has addressed the electric power balance in DD start-up scenario of a tokamak DEMO reactor by extending previous works in system dynamics approach [7,8]. In particular, the current drive power to maintain the required plasma current has been evaluated consistently with spontaneous bootstrap current and temporal evolution plasma temperature. The NBI power of 145 MW is needed to maintain the nominal designed plasma current of 14.0 MA at the beginning of the DD start-up phase while it settles down to 64 MW at the DT steady state.

The electric power demand for the BOP is also inevitable to operate the DEMO plant. Circulating power in the plant is evaluated including cooling and cryogenic systems which are major consumers of electric power. In the reference case, it takes 144 days to reach the DT steady state where DT ratio is 1:1 while the net electric power output becomes positive after 80 days from the start.

In this study, the basic operational condition relies on the steady-state operational scenario with the external current drive. The timescale and the electric energy to ramp-up the plasma current is much shorter and negligibly smaller than those subjected to this study, respectively. In contrast, pulsed operation is attracting interests from mitigation of operational requirements. In principle, the DD start-up scenario is applicable to pulsed operation and its assessment will be a future work.

Tritium cycle is described by stocks, flows and loops in a system dynamics. The time constants determine flows to connect stocks. While these values trace essentially the prior works [7, 8], there are uncertainties in the assumed settings. For example, the timescale of isotope isolation is set at 1800 s in this study (see Fig. 6) and other Ref. [9] suggests 4800 s. When the value of 4800 s is used instead of

1800 s, the number of days to reach the DT steady state and to get the positive net power generation becomes 184 days and 96 days. It should be noted that the DIR can mitigate these gaps.

Options to improve the performance and/or to check the sensitivity of parameters have been investigated for DIR, initial load of T, NBI power constraint and TBR. Wall absorption and recycling of fuels have not been incorporated in the present model. Indeed, several % of wall absorption leads to significant delay of the operational build-up and subsequent significant increase of T inventory in the wall is concerned. Although the present simulations of system dynamics are based upon simplified models, parameter scans are easy to be done and the results from the design study involving sophisticated models and numerical codes are used as a benchmark. With paying attention to uncertainties, the present study suggests the direction and the targets for R&D programs and DEMO design studies.

Acknowledgments

The authors are grateful to valuable comments from Prof. Y. Fujii for electric power generation and Prof. S. Imagawa for a cryogenic system. Informative communications about the specification of JA DEMO with Dr. Y. Sakamoto and Dr. Y. Someya are also deeply acknowledged.

[1] R.J. Pearson *et al*., Fusion Eng. Des. **136**, 1140 (2018).
[2] M. Ni *et al*., Fusion Eng. Des. **88**, 2422 (2013).
[3] I.R. Cristescu *et al*., Nucl. Fusion **47**, S458 (2007).
[4] X. Wang *et al*., Fusion Energy **38**, 125 (2018).
[5] P. Rodriguez-Fernandez *et al*., Nucl. Fusion **62**, 042003 (2022).
[6] S. Konishi *et al*., Plasma Fusion Res. **76**, 1309 (2000).
[7] R. Kasada *et al*., Fusion Eng. Des. **98-99**, 1804 (2015).
[8] K. Miyamae *et al*., Fusion Eng. Des. **160**, 111794 (2020).
[9] C. Day and T. Giegerich, Fusion Eng. Des. **88** 616 (2013).
[10] https://www.iseesystems.com/store/products/stella-architect.aspx
[11] ITER Physics, Nucl. Fusion **39**, 2175 (1999).
[12] Y. Sakamoto *et al*., Fusion Eng. Des. **89**, 2440 (2014).
[13] J. Wesson, *Tokamaks, 4th Edition* (Oxford University Press, Oxford, 2011) Chap. 10.
[14] M.N. Rosenbluth *et al*., Phys. Fluids **15**, 116 (1972).
[15] J.G. Cordey, Plasma Phys. Control. Fusion **26**, 1 (1984).
[16] N.J. Fisch, Rev. Mod. Phys. **59**, 175 (1987).
[17] Y. Miyoshi *et al*., Fusion Eng. Des. **126**, 110 (2018).
[18] E. Fauve *et al*., IOP Conf. Ser.: Mater. Sci. Eng. **171**, 012008 (2017).
[19] P. Sonato *et al*., Nucl. Fusion **57**, 056026 (2017).
[20] A. Simonin *et al*., Nucl. Fusion **55**, 123020 (2015).
[21] R. Sakamoto (National Institute for Fusion Science), private communication.
[22] R. Sakamoto and H. Yamada, Plasma Fusion Res. **4**, 002 (2009).
[23] G. Federici *et al*., Nucl. Fusion **59**, 066013 (2019).
[24] Y. Someya *et al*., Nucl. Fusion **64**, 046025 (2024).